ORIGINAL PAPER
Polish Journal of Microbiology
2022, Vol. 71, No 3, 381–394
https://doi.org/10.33073/pjm-2022-034

Genome-Guided Investigation Provides New Insights into Secondary Metabolites of *Streptomyces parvulus* SX6 from *Aegiceras corniculatum*

NGOC TUNG QUACH[1, 2], THI HANH NGUYEN VU[1, 2], THI LIEN BUI[2], ANH TUAN PHAM[1, 2], THI THU AN NGUYEN[2], THI THANH XUAN LE[2], THI THU THUY TA[3], PRAVIN DUDHAGARA[4] and QUYET-TIEN PHI[1, 2]*

[1] Graduate University of Science and Technology, Vietnam Academy of Science and Technology, Hanoi, Vietnam
[2] Institute of Biotechnology, Vietnam Academy of Science and Technology, Hanoi, Vietnam
[3] Hanoi Open University, Hanoi, Vietnam
[4] Department of Biosciences (UGC-SAP-II and DST-FIST-I), Veer Narmad South Gujarat University, Surat, India

Submitted 16 March 2022, accepted 13 July 2022, published online 19 September 2022

Abstract

Whole-genome sequencing and genome mining are recently considered an efficient approach to shine more light on the underlying secondary metabolites of *Streptomyces*. The present study unearths the biosynthetic potential of endophytic SX6 as a promising source of biologically active substances and plant-derived compounds for the first time. Out of 38 isolates associated with *Aegiceras corniculatum* (L.) Blanco, *Streptomyces parvulus* SX6 was highly active against *Pseudomonas aeruginosa* ATCC® 9027™ and methicillin-resistant *Staphylococcus epidermidis* (MRSE) ATCC® 35984™. Additionally, *S. parvulus* SX6 culture extract showed strong cytotoxicity against Hep3B, MCF-7, and A549 cell lines at a concentration of 30 µg/ml, but not in non-cancerous HEK-293 cells. The genome contained 7.69 Mb in size with an average G + C content of 72.8% and consisted of 6,779 protein-coding genes. AntiSMASH analysis resulted in the identification of 29 biosynthetic gene clusters (BGCs) for secondary metabolites. Among them, 4 BGCs showed low similarity (28–67% of genes show similarity) to actinomycin, streptovaricin, and polyoxypeptin gene clusters, possibly attributed to antibacterial and anticancer activities observed. In addition, the complete biosynthetic pathways of plant-derived compounds, including daidzein and genistein were identified using genome mining and HPLC-DAD-MS analysis. These findings portray an exciting avenue for future characterization of promising secondary metabolites from mangrove endophytic *S. parvulus*.

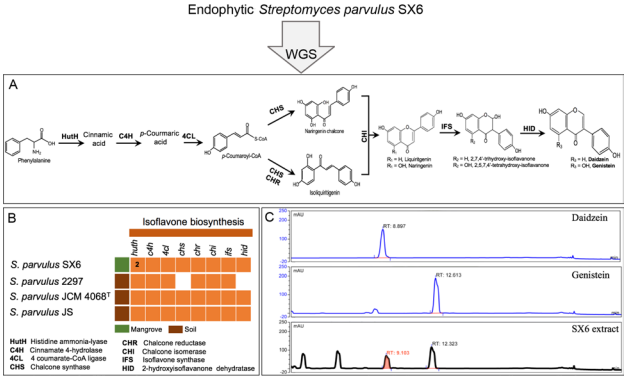

Keywords: *Aegiceras corniculatum*, *Streptomyces parvulus*, genome mining, plant-derived compounds, secondary metabolites

Introduction

Streptomyces is a well-known genus of actinobacteria, capable of producing various bioactive compounds widely used in medicinal and pharmaceutical industries. Terrestrial *Streptomyces* are known to be producers of secondary metabolites with significant biological activities, including antibacterial, anticancer, antioxidant, and anti-inflammatory, contributing to nearly 45% of commercially available antibiotics used by humans (Azman et al. 2017). Since the opportunity of finding novel metabolites has been limited to common terrestrial *Streptomyces* species in the last decades, extreme environmental *Streptomyces* have gained more attention (Lee et al. 2018; Girão et al. 2019). The mangrove is known for its dynamic environment with high salinity, temperature, pH, and fluctuating nutrient availability, from which various *Streptomyces* strains possess

* Corresponding author: Q.-T. Phi, Graduate University of Science and Technology, Vietnam Academy of Science and Technology, Hanoi, Vietnam; Institute of Biotechnology, Vietnam Academy of Science and Technology, Hanoi, Vietnam; **e-mail: tienpq@ibt.ac.vn**
© 2022 Ngoc Tung Quach et al.
This work is licensed under the Creative Commons Attribution-NonCommercial-NoDerivatives 4.0 License (https://creativecommons.org/licenses/by-nc-nd/4.0/).

a wide array of therapeutic drugs that have already been isolated (Tan et al. 2017; Chandrakar and Gupta 2019; Quach et al. 2021).

It is believed that actinobacteria can adapt highly to harsh mangrove conditions by developing unique metabolic pathways, which can provide novel secondary metabolites (Tan et al. 2017). Of note, one of the less explored niches in the mangrove environments is the mangrove plants such as *Aegiceras corniculatum*. A previous study reported that *Streptomyces* sp. GT-20026114 from *A. corniculatum* produced four novel cyclopentene derivatives; however, antimicrobial, anticancer, and antiviral activities were not detected (Wang et al. 2010). It raises the possibility of finding new bioactive compounds from endophytic *Streptomyces*.

Instead of traditional methods that have considerably slowed the chance of finding new compounds, whole-genome sequencing and genome mining have paved a new way to exploit the biosynthetic potential of bioactive *Streptomyces*. Comparative genome studies demonstrated that *Streptomyces* species had an open genome in which biosynthetic gene clusters (BGCs) accounted for 15% of the genome size (Tian et al. 2016; Chevrette and Currie 2019). Interestingly, *Streptomyces fildesensis* and *Streptomyces bingchenggensis* devoted 22% of their genomes to BGCs (Núñez-Montero et al. 2019; Belknap et al. 2020).

In addition, most BGCs remain poorly characterized and are silent under laboratory culture conditions. A novel anti-HIV compound streptoketides from soil *Streptomyces* sp. Tü 6314 was recently discovered by identifying a cryptic type II PKS cluster predicted by antiSMASH (Qian et al. 2020). In addition, genome analysis of *S. coelicolor* A3(2) found bacterial homologous genes of a plant-derived enzyme involved in isoflavonoid synthesis (Moore et al. 2002). Isoflavonoids such as genistein and daidzein are polyphenolic secondary metabolites in plants, which are believed to have anticancer, antibacterial, and antioxidant activities (Liu et al. 2021; Sohn et al. 2021). Surprisingly, endophytic *Streptomyces* spp. such as *Streptomyces variabilis* LCP18, *Streptomyces* sp. YIM 65408, and *Streptomyces cavourensis* YBQ59 also produced either active genistein or daidzein in the cultural broth (Yang et al. 2013; Vu et al. 2018; Quach et al. 2021).

However, genes encoding functional proteins involved in the biosynthesis of these plant-derived compounds have not been exploited yet. More and more *Streptomyces* genomes publicly available would increase opportunities for identifying novel and existing BGCs, avoiding time-consuming and labor-intensive experiments.

In this study, we characterized biological activities and sequenced the genome of *Streptomyces parvulus* SX6 associated with *A. corniculatum* collected in the mangrove forest area of Quang Ninh province, northern Vietnam, where studies on actinobacteria and their bioactive metabolites are scanty. Given that only three terrestrial *S. parvulus* are available from the NCBI, this is the first genomic report of mangrove endophyte *S. parvulus* showing BGCs attributed to remarkable antibacterial and anticancer activities. In addition, the biosynthetic pathway of plant-derived compounds, including daidzein and genistein, was proposed using comparative genomic and HPLC-DAD-MS analysis. These findings highlight the capability of endophytic *Streptomyces* from mangrove plants to produce novel agents and plant-derived compounds with therapeutic applications.

Experimental

Materials and Methods

Collection and isolation of endophytic actinobacteria. The roots, stems, and leaves of healthy mangrove plants *A. corniculatum* were collected from different sites in Quang Ninh province (21.0064°N, 107.2925°E), Vietnam, in June 2020. These samples were placed in sterile plastic bags, transported to the laboratory, and used for isolation procedures within 48 h. The obtained plants were then identified as *A. corniculatum* species by the Institute of Ecology and Biological Resources, Vietnam Academy of Science and Technology. The samples were washed with tap water and distilled water. The surface sterilization procedure was carried out as described previously to eliminate unwanted microorganisms (Musa et al. 2020; Vu et al. 2020). The sterilized samples were frozen at −80°C for 2 weeks and spread onto 8 media, including humic acid-vitamin B agar (humic acid 1.0 g/l, Na_2HPO_4 0.5 g/l, KCl 1.7 g/l, $MgSO_4 \cdot 7H_2O$ 0.05 g/l, $CaCl_2$ 1.0 g/l, vitamins mixture 1.0 g/l, agar 15.0 g/l, pH 7.0), raffinose-histidine agar (histidine 0.5 g/l, raffinose 2.5 g/l, K_2HPO_4 1.0 g/l, $MgSO_4 \cdot 7H_2O$ 0.5 g/l, $FeSO_4 \cdot 7H_2O$ 0.01 g/l, $CaCl_2$ 0.02 g/l, agar 15.0 g/l, pH 7.0), tap water-yeast agar (yeast 0.25 g/l, K_2HPO_4 0.5 g/l, agar 15.0 g/l, pH 7.2), trehalose-proline agar (trehalose 5.0 g/l, proline 1.0 g/l, $(NH_4)_2SO_4$ 1.0 g/l, NaCl 1.0 g/l, $CaCl_2$ 2.0 g/l, K_2HPO_4 1.0 g/l, $MgSO_4 \cdot 7H_2O$ 1.0 g/l, agar 15.0 g/l, pH 7.0), sodium succinate-asparagine agar (sodium succinate 1.0 g/l, L-asparagine 1.0 g/l, KH_2PO_4 0.9 g/l, K_2HPO_4 0.6 g/l, $MgSO_4 \cdot 7H_2O$ 0.1 g/l, $CaCl_2$ 0.2 g/l, KCl 0.3 g/l, $FeSO_4 \cdot 7H_2O$ 0.001 g/l, agar 15.0 g/l, pH 7.2), starch agar (starch 20 g/l; KNO_3 2 g/l, K_2HPO_4, 1.0 g/l, $MgSO_4 \cdot 7H_2O$ 0.5 g/l, NaCl 0.5 g/l, $CaCO_3$ 3.0 g/l, $FeSO_4 \cdot 7H_2O$ 0.01 g/l, agar 15.0 g/l, pH 7.0), citrate acid agar (citric acid 0.12 g/l, $NaNO_3$ 1.5 g/l, K_2HPO_4 0.4 g/l, $MgSO_4 \cdot 7H_2O$ 0.1 g/l, $CaCl_2$ 0.05 g/l, EDTA 0.02 g/l, Na_2CO_3 0.2 g/l, agar 15.0 g/l, pH 7.2), and sodium propionate agar (sodium propionate 1.0 g/l, L-asparagine

0.2 g/l, KH_2PO_4 0.9 g/l, K_2HPO_4 0.6 g/l, $MgSO_4 \cdot 7H_2O$ 0.1 g/l, $CaCl_2$ 0.2 g/l, agar 15.0 g/l, pH 7.0) as described previously (Qin et al. 2009; Musa et al. 2020; Vu et al. 2020). Each medium was amended with 50 mg/ml nystatin, 25 mg/ml $K_2Cr_2O_7$, and 25 mg/ml nalidixic acid to inhibit the growth of Gram-negative bacteria and fungi. All plates were incubated for one month at 30°C. Once observed, actinobacteria colonies were purified by repeated streaking onto International Streptomyces Project (ISP) 2 medium (Quach et al. 2021) and then stored in 15% (v/v) glycerol at –80°C.

Morphological characteristics and molecular identification by 16S rRNA phylogenetic analysis. Morphological and physical characteristics of the bioactive isolate were studied using a series of ISP1-ISP7 agar media. The morphological features were observed using a scanning electron microscope (SEM) JSM-5410 (JEOL, Japan). To evaluate the effect of pH, strain SX6 were grown in ISP2 medium at pH 2.0–10.0 adjusted with different buffer systems including 0.1 M KCl/0.02M HCl pH 2.0; 0.1 M citric acid/0.1 M sodium citrate pH 3.0–5.0; 0.1 M KH_2PO_4/0.1 M NaOH pH 6.0–8.0; 0.1 M $NaHCO_3$/0.1 M Na_2CO_3 pH 9.0–10.0 (Singh et al. 2019). Growth at different NaCl concentrations (0–10%, w/v) and varying temperature conditions (15–45°C) was performed as described previously (Quach et al. 2021). The ability to utilize sole carbon and nitrogen sources was assessed using the basal medium described previously (Williams et al. 1983). The enzymatic tests such as amylase, cellulase, chitinase, protease, and xylanase were performed on the ISP2 agar medium (Quach et al. 2021).

Following the manufacturer's protocol, the genomic DNA of strain SX6 was extracted using G-spin™ Total DNA Extraction Mini Kit (Intron Bio, Korea). PCR amplification for the 16S rRNA gene was performed as described previously (Quach et al. 2021). The identification of phylogenetic neighbors and calculation of pairwise 16S rRNA gene sequence similarities were carried out on the EzTaxon server (Chun et al. 2007). The phylogenetic tree was built by the maximum-likelihood method using Molecular Evolutionary Genetics Analysis (MEGA) software version 7 with Kimura-2-parameter distances. *Nocardia farcinica* ATCC® 3318™ (NR_115831) was used as an outgroup branch. The obtained 16S rRNA gene sequence was deposited at GenBank (NCBI) under accession number OL468549.

Inhibitory effects of strain SX6 on pathogenic bacteria. All endophytic actinobacteria were cultivated in an ISP2 medium at 30°C with shaking at 180 rpm for 8 days. Agar-well dilution assay was used to evaluate antimicrobial activity against 6 pathogenic bacteria, including *Bacillus cereus* ATCC® 11778™, *Pseudomonas aeruginosa* ATCC® 9027™, methicillin-resistant *Staphylococcus epidermidis* (MRSE) ATCC® 35984™, *Enterobacter aerogenes* ATCC® 13048™, *Escherichia coli* ATCC® 11105™, *Salmonella typhimurium* ATCC® 14028™ (Holder and Boyce 1994). All test bacteria were grown in Luria-Bertani (LB) medium and then spread on the entire surface of LB agar plates. Six mm (diameter) wells were perforated in the agar, in which 100 µl of cell-free supernatant was added to each well. The experiment was performed in triplicates, and diameters of inhibition zones were determined after 12–16 h of incubation at 37°C. Heatmap illustrating the antibacterial activity of endophytic isolates was generated through the online software Heatmapper (Babicki et al. 2016).

Ethyl acetate was used to extract secondary metabolites from strain SX6 following the procedure described previously (Nguyen et al. 2019b). In brief, the mixture of cell-free supernatant:ethyl acetate (1:1 ratio) was vigorously shaken for 30 min and kept stationary 60 min until the separation of aqueous and organic phases. The organic phase was evaporated on the rotary evaporator (Scilogex RE100-Pro, USA) at 55°C and 80 × *g*. The dried crude extract was weighed and dissolved in DMSO or 70% ethanol, depending on the experiments. The crude extract of SX6 was evaluated for its antibacterial activity using the minimum inhibitory concentration (MIC) (Andrews 2001). MIC values were recorded as the lowest concentration with no visible growth of pathogenic bacteria after 12–16 h of incubation.

Cytotoxic activity. Cytotoxicity against human hepatoma Hep3B, breast cancer MCF-7, lung cancer A549, and non-cancerous HEK-293 cell lines was assessed by 3-(4,5-dimethythiazol-2-yl)-2,5-diphenyl tetrazolium bromide (MTT) assay (Salam et al. 2017). Briefly, the Hep3B, MCF-7, A549, and HEK-293 cell lines were seeded in 96-well plates containing RMPI medium supplemented with 10% fetal bovine serum, 100 U/ml penicillin, and 100 µg/ml streptomycin at a density of ~2.5×10^4 cells/well and then incubated at 37°C, 5% CO_2 for 48 h. Then, the cells were exposed to 30 µg/ml and 100 µg/ml of SX6 extract. After 24 h of incubation, 20 µl of MTT (5 mg/ml in PBS) was added to each well, followed by incubation at 37°C, 5% CO_2 for 4 h. The medium was discarded by gentle aspiration, and the formazan crystals were dissolved in DMSO. About 10 µg/ml ellipticine was employed as a positive control, while 10% DMSO (v/v) was considered a negative control. The absorbance of each well was measured at 570 nm, and the test was performed in three independent experiments.

The hydroxyl radical scavenging activity. The hydroxyl radical scavenging activity of SX6 extract was evaluated with slight modifications (Liu et al. 2009; Vu et al. 2021). About 1.0 ml of 70% ethanol extract was added to the mixture containing 1.0 ml of 0.75 mM 1,10-phenanthroline, 1.0 ml of 0.75 mM $FeSO_4$, 1.0 ml of 0.01% H_2O_2, and 1.5 ml of 0.15 M sodium phosphate buffer (pH 7.4). The absorbance was measured

at 536 nm, and hydroxyl radical scavenging activity was calculated as follows:

$$Scavenging\ activity\ (\%) = \frac{(A_{sample} - A_{blank})}{(A_0 - A_{blank})} \times 100 \quad (1)$$

where A_{sample} is the absorbance of the mixture containing SX6 extract, A_0 is the absorbance of the reaction mixture without SX6 extract and H_2O_2 (SX6 extract and H_2O_2 were replaced by the same volume of 70% ethanol and distilled water, respectively), and A_{blank} is the absorbance of 70% ethanol.

DPPH-radical scavenging activity. The 2-diphenyl-1-picrylhydrazyl (DPPH) assay was carried out as in the previous studies (Kadaikunnan et al. 2015; Vu et al. 2021). The crude extract dissolved in 70% ethanol was reacted with 0.2 ml of 0.1 mM 2,2-diphenyl-1-picrylhydrazyl (DPPH) followed by 2.0 ml of deionized water. The reaction was incubated in the dark for 30 min, and absorbance was subsequently measured at 517 nm. The following formula was used to calculate the percentage DPPH radical scavenging activity of SX6 extract:

$$Scavenging\ activity\ (\%) = 1 - \frac{(A_{sample} - A_0)}{A_{blank}} \times 100 \quad (2)$$

where A_{sample} is the absorbance of the mixture comprising SX6 extract, A_0 is the absorbance of 70% ethanol and 0.1 mM DPPH solution, and A_{blank} is the absorbance of 70% ethanol.

Whole-genome sequencing, *de novo* assembly, and annotation. The whole genome was sequenced with the Illumina Miseq sequencing platform (Illumina, USA). The quality control was performed by FastQC (http://www.bioinformatics.babraham.ac.uk/projects/fastqc), and read trimming was implemented using Trimmomatic 3.0 (Bolger et al. 2014). SPAdes 3.13 was used for *de novo* assembly with default parameters and k-mer = 21, 33, 55, 77 (Bankevich et al. 2012). The completeness of the assembled genome was evaluated using the Benchmarking Universal Single-Copy Orthologous (BUSCO) v3.0 (https://gitlab.com/ezlab/busco). The SX6 genome was annotated by Prokaryotic Genomes Annotation Pipeline (http://www.ncbi.nlm.nih.gov/genome/annotation_prok), Prokka (Seemann 2014), and Rapid Annotation using Subsystem Technology (RAST) (Aziz et al. 2008). Orthologous genes were analyzed using clusters of orthologous genes (COGs) (Galperin et al. 2015). A whole-genome-based taxonomic analysis (https://tygs.dsmz.de) was utilized to calculate *in silico* digital DDH (dDDH), branch lengths, and genome BLAST distance phylogeny (Meier-Kolthoff and Göker 2019). The genome sequence of *S. parvulus* SX6 were deposited at GenBank under accession number JAJJMU010000000.

Identification of genetic determinants involved in biological activities. Genome mining for BGCs encoding secondary metabolites was performed using antiSMASH 5.1.2 with default parameters and all features selected (Blin et al. 2017). BLASTP and TBLASTN were utilized to determine homologous protein-coding sequences present in SX6 and other *S. parvulus* genomes available on GenBank, including 2297 (CP015866), JCM 4068 (BMRX00000000), and LP03 (JAIWPL000000000).

HPLC-DAD-MS analysis of plant-derived compounds. The SX6 extract samples were analyzed on a Thermo Dionex Ultimate 3000 HPLC system (Thermo Fisher Scientific, USA) consisting of a vacuum degasser, a quaternary mixing pump, an autosampler, a column oven, and a diode-array detector (DAD), which was coupled to a Thermo MSQ Plus single quadrupole mass spectrometer (Thermo Fisher Scientific, USA). A Hypersil GOLD HPLC column (150 mm × 4.6 mm, 5 μm) was used at 35°C in which 0.1% formic acid in HPLC grade water (Fisher Scientific, USA) and acetonitrile (Fisher Scientific, USA) were set as solvent channels A and B, respectively. The crude SX6 extract (5 mg/ml) dissolved in methanol HPLC grade was injected at a flow rate of 400 μl/min with an injection volume of 2 μl and a UV detector at 254 nm. Daidzein and genistein present in the crude SX6 extract were detected by comparing the retention times and UV spectra with the reference compounds of daidzein and genistein (Sigma, USA) under the same HPLC condition. Moreover, MS spectra were used to confirm the ion of daidzein at m/z 255 ($[M+H]^+$) and genistein at m/z 271 ($[M+H]^+$) as described previously (Shrestha et al. 2021).

Results

Screening of bioactivity and identification of the isolate SX6. A total of 38 actinobacteria with different morphological characteristics were isolated from the mangrove plant *A. corniculatum*. Primary screening of antibacterial activity against six selective pathogens revealed that 27 isolates were active against at least one tested bacterium. Using the 16S rRNA sequence analysis, 21 out of 27 isolates were affiliated with the genus *Streptomyces* (Table SI). Among them, isolate SX6 displayed significant broad-spectrum antibacterial effects on five tested pathogens (Fig. 1). Indeed, SX6 isolated from stems depicted inhibition zones against *S. typhimurium* ATCC® 14028™ (16.0 ± 0.4 mm), *E. coli* ATCC® 11105™ (7.9 ± 0.1 mm), *P. aeruginosa* ATCC® 9027™ (23.6 ± 0.6 mm), MRSE ATCC® 35984™ (32.5 ± 0.1 mm), and *E. aerogenus* ATCC® 13048™ (12.4 ± 0.1 mm).

When grown on ISP1-7 media, the aerial mycelium of isolate SX6 formed monopodial branched hyphae and was well-developed with white color, while substrate

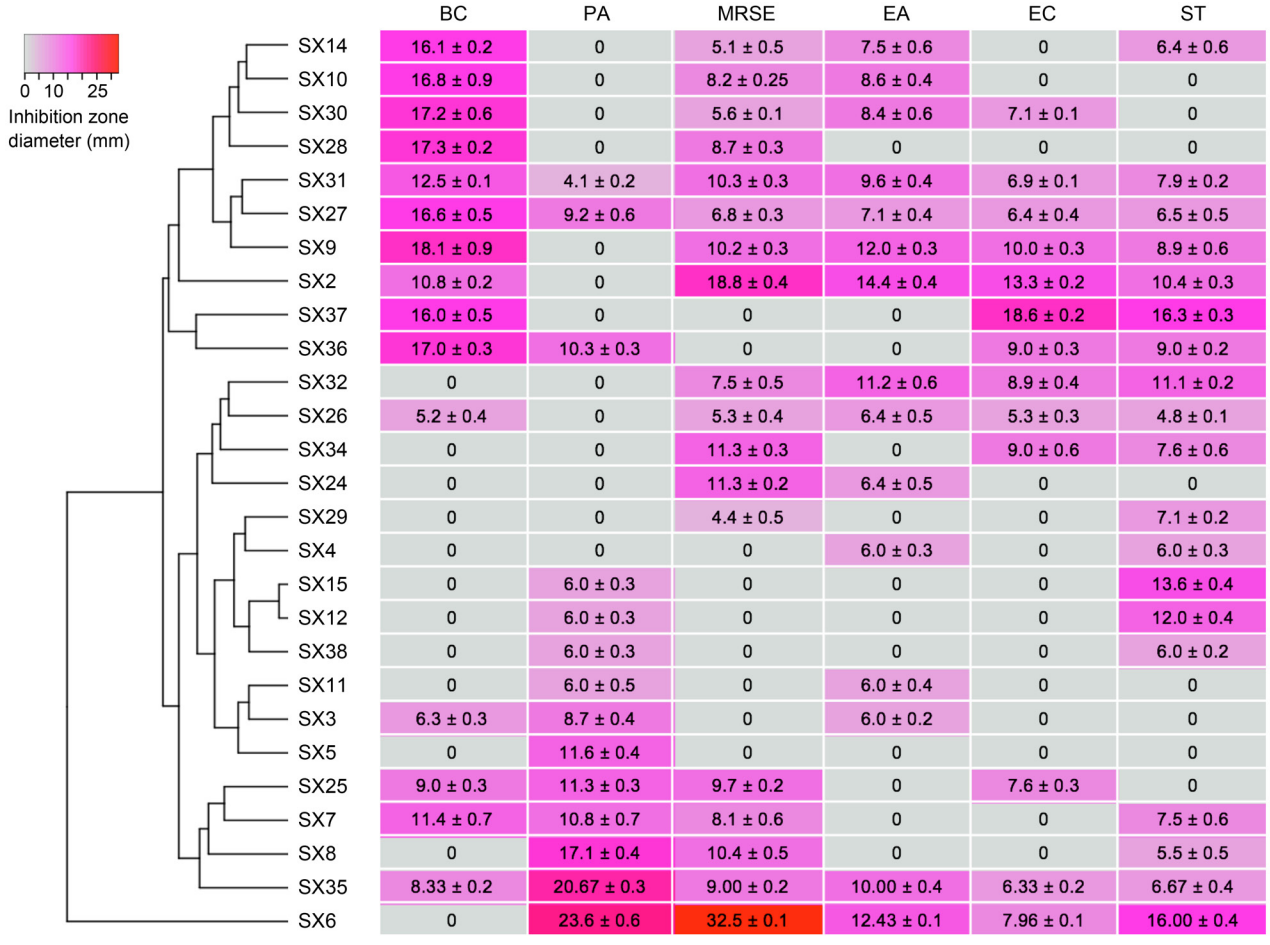

Fig. 1. Heatmap presenting antibacterial activity against at least one tested pathogenic bacteria of endophytic actinobacteria isolated from *Aegiceras corniculatum*.

BC – *Bacillus cereus* ATCC® 11778™, PA – *Pseudomonas aeruginosa* ATCC® 9027™, MRSE – methicillin-resistant *Staphylococcus epidermidis* ATCC® 35984™, EA – *Enterobacter aerogenes* ATCC® 13048™, EC – *Escherichia coli* ATCC® 11105™, ST – *Salmonella typhimurium* ATCC® 14028™.

mycelium was pale yellow (Table SII). The yellow pigment was observed in the ISP2 agar on which this isolate grew at the maximum level under cultivation temperature of 30°C, pH 7.0, and 1% NaCl. Spiral spore chain and warty spore surface were observed by SEM (Fig. 2A). In addition, the isolate SX6 assimilated various carbon sources such as glucosamine, fructose, sorbitol, trehalose, mannose but not myo-inositol, mannitol, and raffinose. Enzymatic tests revealed the production of cellulase, chitinase, protease, and xylanase (Table SII).

BLAST search of the 16S rRNA gene sequence of SX6 showed the highest similarity to *S. parvulus*

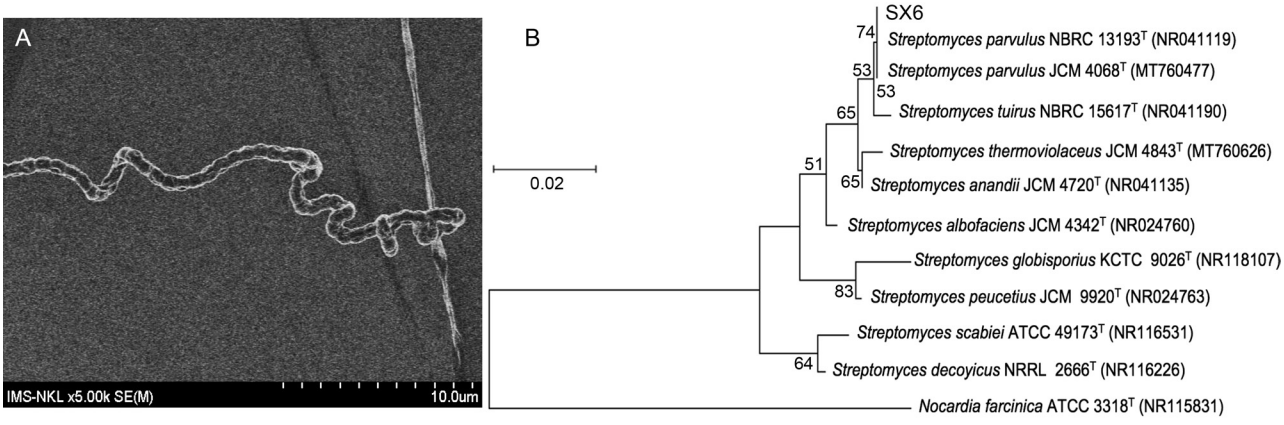

Fig. 2. Identification of endophytic strain SX6.

A) Scanning electron microscopy of hyphae of strain SX6 grown on ISP2 medium; B) phylogenetic tree based on 16S rRNA gene sequences of strain SX6 and closely related *Streptomyces* strains.

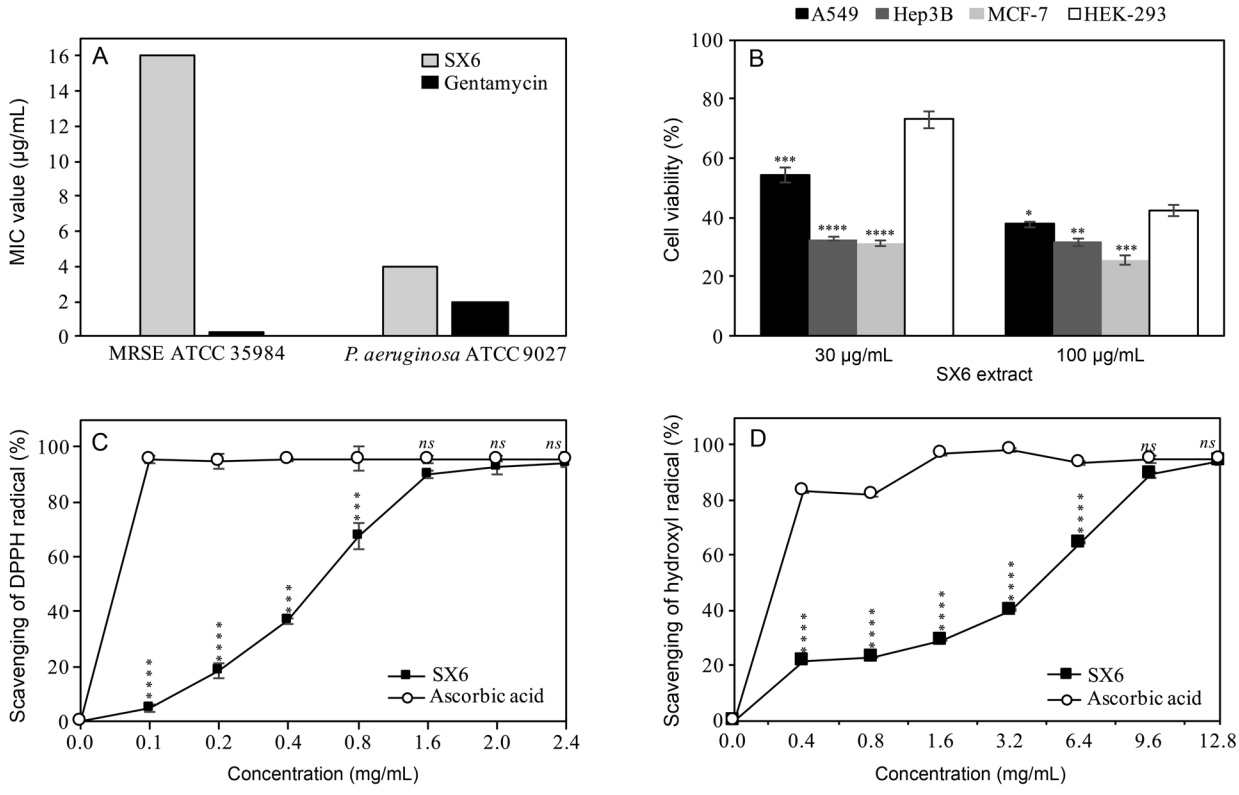

Fig. 3. Biological activities determined in the *Streptomyces parvulus* SX6 extract.

A) Selective antibacterial activity against MRSE ATCC® 35984™ and *Pseudomonas aeruginosa* ATCC® 9027™; B) cytotoxic activity against A549, Hep3B, MCF-7, and HEK-293 cell lines; C) and D) antioxidant activities, including DPPH free radical scavenging and hydroxyl radical scavenging were determined in the SX6 extract. Mean values and SD of three independent experiments are shown and *p*-values were calculated by the Student's unpaired two-tailed *t*-test by the graph prism software ($^{ns}p > 0.05$, $^{*}p < 0.05$, $^{**}p < 0.01$, $^{***}p < 0.001$, and $^{****}p < 0.0001$).

NBRC 13193 (100%) and *S. parvulus* JCM 4068 (99.9%). In addition, the neighbor-joining phylogenetic tree indicated that isolate SX6, *S. parvulus* NBRC 13193 and *S. parvulus* JCM 4068 were located on the same branch of the tree (Fig. 2B). Morphological, biochemical characteristics and 16S rRNA gene sequence analyses confirmed the mangrove endophytic strain SX6 as *Streptomyces parvulus* SX6.

Evaluation of antibacterial, antioxidant, and anticancer activities of *S. parvulus* SX6 extract. In the antibacterial assay, the SX6 extract displayed superior activity against only *P. aeruginosa* ATCC® 9027™ and MRSE ATCC® 35984™ with MIC values of 4 µg/ml and 16 µg/ml, respectively (Fig. 3A). Regarding *in vitro* cytotoxicity effects on human cell lines, the SX6 extract had significant inhibition at both concentrations with the viability of 3 cell lines ranging from 25.6–54.2% (Fig. 3B). Specifically, 30 µg/ml extract displayed the highest cytotoxic activity against MCF7 and Hep3B with cell viability recorded at 31.1 ± 0.8% and 32.7 ± 0.8%, respectively. Increasing extract concentration to 100 µg/ml did not significantly enhance cytotoxic activity against MCF7 and Hep3B cell lines. In contrast, A549 was resistant to 30 µg/ml extract but not to 100 µg/ml at which concentration cell viability decreased to less than 40%. Meanwhile, the SX6 extract showed low cytotoxicity against non-cancerous cell line HEK-293 with cell viability of 72.9 ± 2.6% and 42.5 ± 1.8% at 30 µg/ml and 100 µg/ml extract, respectively.

DPPH and hydroxyl radical scavenging assays *in vitro* presented significant antioxidant effects of the SX6 extract (Fig. 3C). To be specific, the SX6 extract proved the most potent antioxidant activity against DPPH free radicals (90.0 ± 1.4%) at 1.6 mg/ml, which was comparable to that of the ascorbic acid ($p > 0.05$). Moreover, the hydroxyl radical scavenging activity of the SX6 extract was determined to be 89.1 ± 0.9% at 9.6 mg/ml, similar to the activity of ascorbic acid ($p > 0.05$) (Fig. 3D).

General genomic features and comparative genomes. To deeper understand the biological properties of *S. parvulus* SX6, this strain was sequenced by the Illumina platform. A total of 5,733,880 high-quality reads were generated, yielding a 7.69 Mb linear chromosome with an average G + C content of 72.8% (Table I). The chromosome contained 48 contigs encoding for 6,779 protein-coding genes (CDSs). The genome assembly was validated using BUSCO, leading to 135 complete single-copy (91.22%), seven duplicated (4.73%), five missing (3.38%), and one fragmented (0.68) BUSCOs.

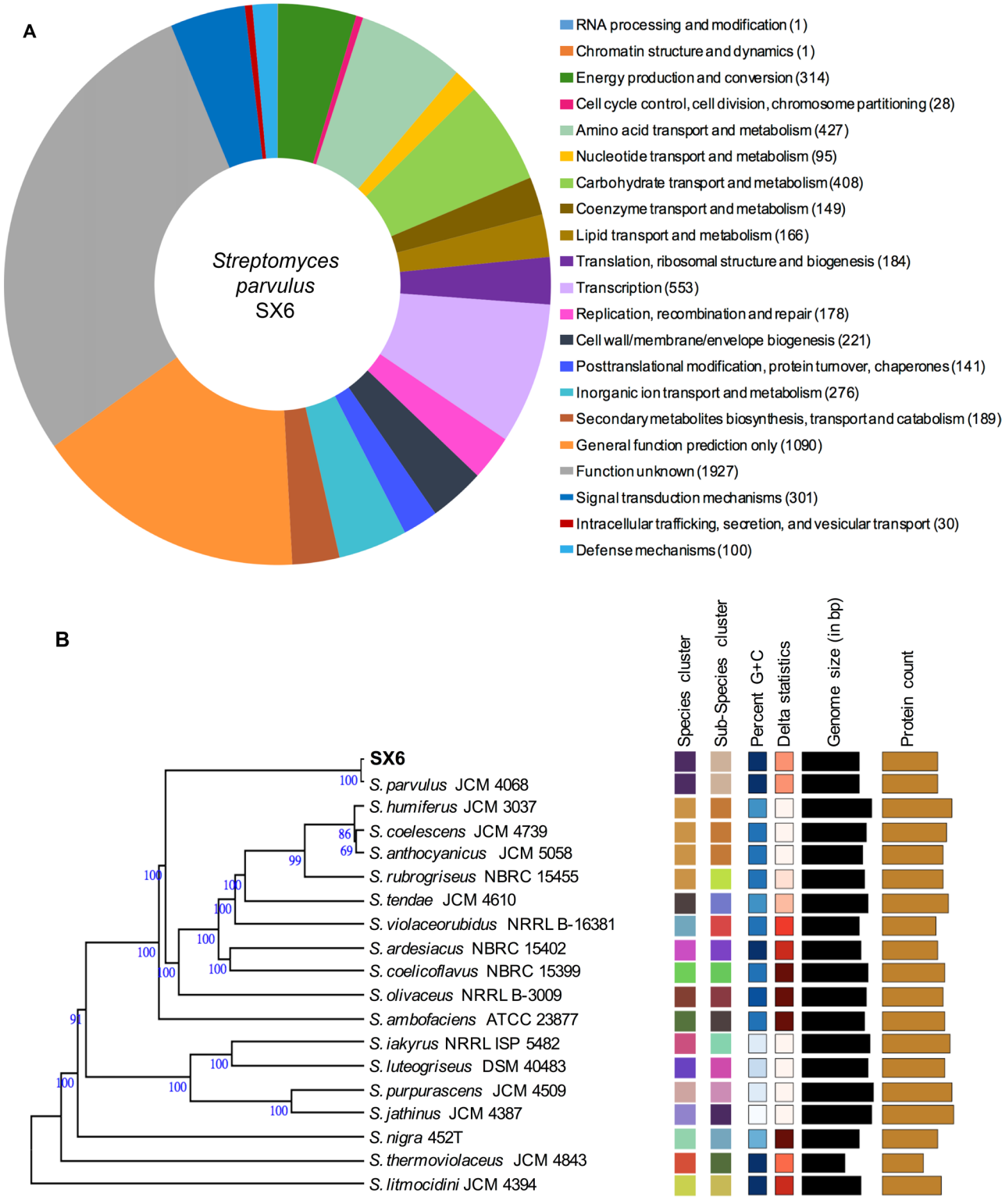

Fig. 4. Genome characterization of *Streptomyces parvulus* SX6.

A) Clusters of Orthologous Groups (COGs) of protein functions; B) whole genome-based phylogenetic classification of *S. parvulus* SX6. The numbers on the branches are GBDP pseudo-bootstrap support values of > 60% from 100 replications, with average branch support of 96.6%.

For functional annotation, 6,779 CDSs (99.2%) were assigned to 21 functional categories. Almost all CDSs were associated with functions, including general function (1,090 genes), transcription (553 genes), amino acid transport and metabolism (427 genes), carbohydrate transport and metabolism (408 genes), and energy production and conversion (314 genes) (Fig. 4A).

The species status of strain SX6 was further confirmed by *in silico* dDDH and G + C difference values. Among 18 reference strains, SX6 showed the highest

Table I
Features of the SX6 and other *Streptomyces parvulus* genomes.

Species	Size (Mb)	GC (%)	Genes	CDSs	tRNAs	rRNAs
S. parvulus SX6	7.69	72.8	6,952	6,779	68	11
S. parvulus JCM 4068	7.69	71.5	6,881	6,866	66	3
S. parvulus 2297	7.15	72.7	6,951	6,773	66	18
S. parvulus LP03	7.74	72.5	7,030	6,832	66	3

similarity to *S. parvulus* JCM 4068 with *in silico* dDDH and G+C difference values of 94.7% and 0.02%, respectively (Fig. 4B). This finding was in agreement with 16S rRNA sequence analysis, which concluded that the studied strain was *S. parvulus*.

Biosynthetic gene clusters for secondary metabolites of *S. parvulus* SX6. AntiSMASH analysis resulted in the identification of 29 gene clusters encoding secondary metabolites with multiple clusters encoding terpenes (5); non-ribosomal peptide synthetases (NRPS) (9); lantipeptide (1); type II polyketide synthase (T2PKS) (1); type III polyketide synthase (T3PKS) (1); ectoine (1); ribosomally synthesised and post-translationally modified peptide (RiPP) (2); bacteriocin (1); indole (1); siderophore (3); melanin (1); and clusters with a hybrid character (3) (Table SIII).

Six gene clusters, including geosmin, albaflavenone, isorenieratene, hopene, sapB, and ectoine were identified comprising 100% of the genes from the know cluster. Clusters with 60–90% similarity included melanin (60%), citrulassin (60%), spore pigment (66%), desferrioxamin (83%), and coelichelin (90%) (Table SIII). Notably, cluster 2 with a predicted similarity of 67% to BGC of actinomycin D, a well-known antibiotic with high antibacterial and cytotoxic activities (Liu et al. 2016), was a hybrid cluster containing 11 genes homologous to *acmB*, *acnT*, *acmF*, *acmG*, *acmH*, *acmI*, *acmJ, acmU, acmW, acmX,* and *acmrC* (Fig. 5). Another predicted actinomycin D cluster with a lower similarity of only 28% was cluster 20, which consisted of five genes homologous to *acmB, acmA, acmD, acmR, acnT* (24,1 kb) (Fig. 5). Despite being classified as *S. parvulus*, actinomycin D cluster was only found in the genome of soil-derived strain 2297 with 82% similarity, but not in JCM 4068.

In addition, the largest cluster in the SX6 genome, cluster 19, showed moderate similarity at 48% to the BGC of streptovaricin from *S. spectabilis* CCTCC M2017417, encoding 10 PKS and 1 NRPS proteins, and a dozen of other enzymes such as cytochrome P450, transporters, and regulatory proteins (Fig. 5). It is worthy to note that cluster 19 had two repeats of the PKS core biosynthesis genes. Comparative genomics analysis revealed that streptovaricin cluster was not present in the 2297 genome.

Cluster 25 was predicted as a complex of NRPS, T1PKS, and other genes that also exhibited a similarity of 48% with the known polyoxypeptin BGC of *Streptomyces* sp. MK498-98F14 (Fig. 5). Different to polyoxypeptin cluster from *Streptomyces* sp. MK498-98 F14, only 30 genes in cluster 25 were not annotated to the known BGCs. Meanwhile, three cytochrome P450 genes were also found. A polyoxypeptin cluster of 390,736 bp was also predicted in the genome of soil-derived *S. parvulus* 2297 with 51% similarity consisting of three major PKS regions and two NRPS regions. Compared to *S. parvulus* 2297, cluster 25 was around three times smaller and only showed 39% similarity to corresponding BGC.

The biosynthesis of plant-derived compounds. The search for critical enzymes involved in the biosynthesis of plant-derived compounds found nine putative homologous proteins in the SX6 genome, that are not clustered in an operon (Fig. 6A). In the phenylpropanoid pathway, phenylalaline as a precursor for the biosynthesis of daidzein and genistein, is initially catalyzed by phenylalaline ammonia-lyase HutH (*orf_4806, orf_6344*), cinnamate 4-hydrolase C4H (*orf_2463*), 4-coumarate-CoA ligase 4CL (*orf_5768*) yielding p-coumaroyl-CoA . After that, chalcone synthase CHS (*orf_6560*) is responsible for further condensation of p-coumaroyl-CoA to naringenin chalcone in the genistein pathway, while the addition of 3X malonyl-CoA and chalcone reductase CHR (*orf_01094*) result in the conversion of p-coumaroyl-CoA to liquiritigenin that is critical for the daidzein pathway. These intermediates are modified by chalcone isomerase (*orf_3461*) and converted to 2, 7, 4'-trihydroxyl-isoflavanone or 2, 5, 7, 4'-tetrahydroxy-isoflavanone. Finally, isoflavones daidzein and genistein are synthesized under activation of 2-hydroxyisoflavanone dehydratase HID (*orf_01718*) (Fig. 6A). Comparative genome analysis revealed that these genes are also conserved among *S. parvulus* species including JCM 4068, 2297 and LP03. The only exception was *S. parvulus* 2297 in which genes *chr* and *hid* were not found (Fig. 6B). Of note, only SX6 possesses two copies of *hutH*, unlike a single copy of *huth* in the other *S. parvulus* genomes.

In supporting of the genomic finding, HPLC-DAD--MS analysis revealed the presence of daidzein in the

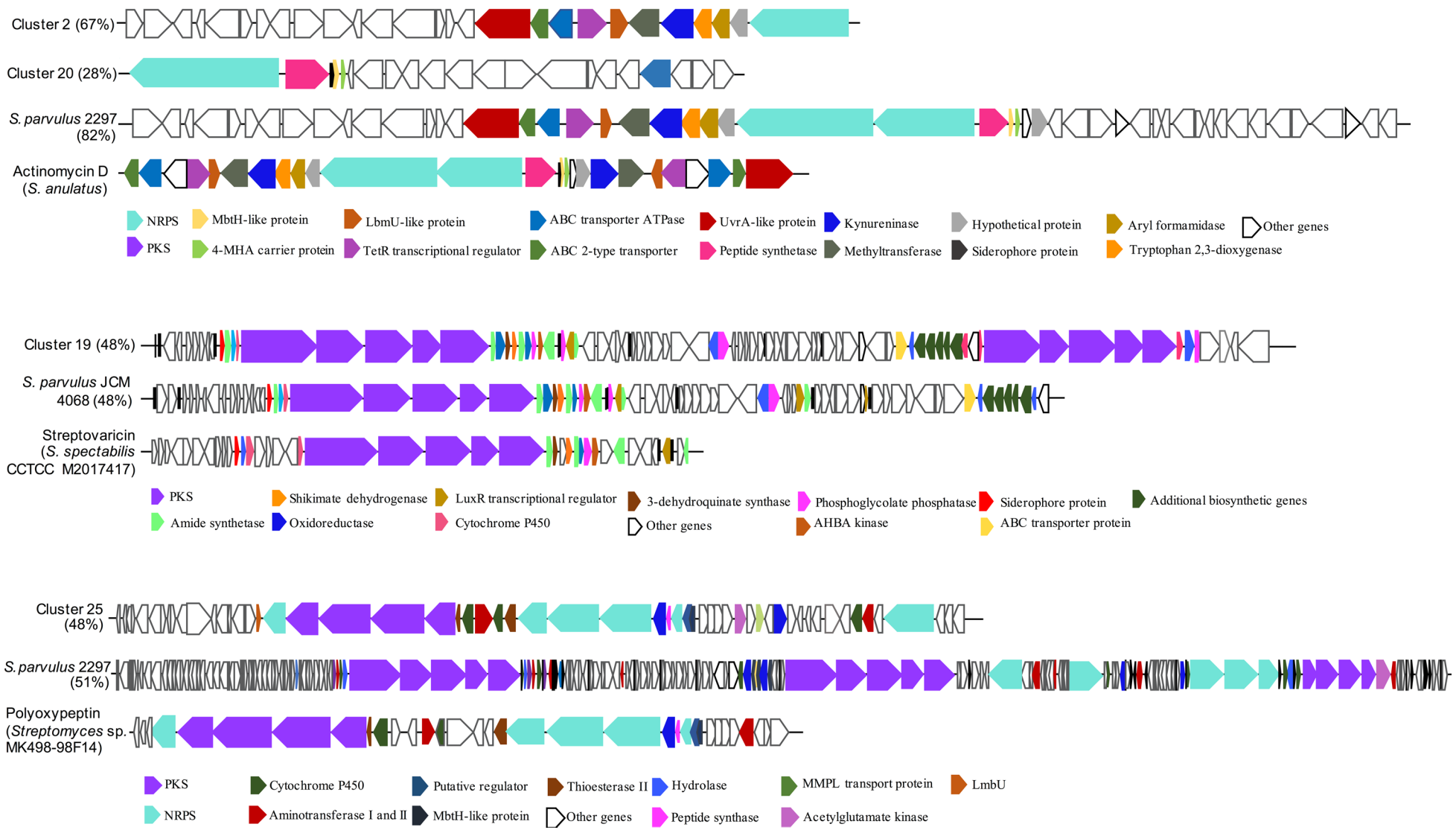

Fig. 5. Cryptic secondary metabolite biosynthetic gene clusters identified in the genome of *Streptomyces parvulus* SX6.

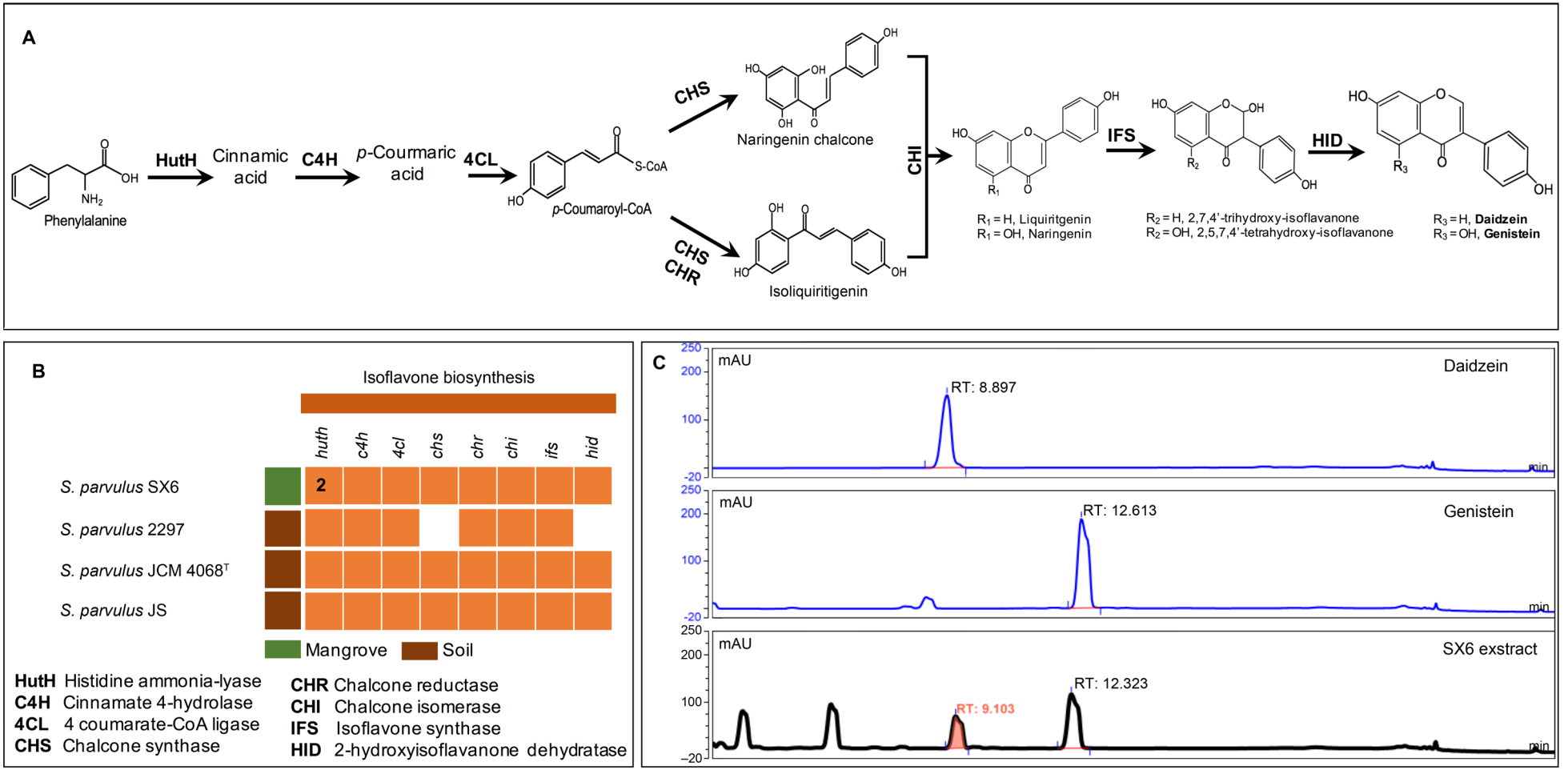

Fig. 6. Biosynthetic pathway of daidzein and genistein in *Streptomyces parvulus* SX6.

A) Using genome mining, the proposed biosynthetic pathways of daidzein and genistein present in *S. parvulus* SX6; B) identification of genes involved in daidzein and genistein biosynthesis across *S. parvulus* genomes; C) HPLC-DAD-MS chromatogram of reference compounds and the extract of mangrove endophytic *S. parvulus* SX6.

extract of SX6 at the retention time of 9.103 min, which was relatively similar to the retention time of the standard daidzein compound (8.897 min) (Fig. 6C). Additionally, genistein was detected based on a 12.323-min retention time. Further confirmation by MS analysis showed that MS spectra of SX6 extract revealed two distinct MS peaks $[M+H]^+ = 255.44$ m/z and $[M+H]^+ = 271.40$ m/z, corresponding to standard daidzein and genistein (Fig. SI and SII). The UV absorption spectra for the SX6 extract also displayed similar peaks with standard daidzein and genistein.

Discussion

The strain SX6 belongs to the *S. parvulus*, as our results demonstrate. Phylogenetic tree based on 16S rRNA gene and whole-genome sequence showed that SX6 formed a distinct cluster with the reference sequences of *S. parvulus* species. *S. parvulus* is mainly isolated from soils, which a producer of actinomycin D with broad-spectrum activities against bacteria, fungi, viruses, and cancer cells (Shetty et al. 2014; Chandrakar and Gupta 2019). The earlier genomic analysis claimed that *S. parvulus* 03 from mangrove plant *Kandelia candel* potentially secreted friulimicin, lobophorin, laspartomycin, colabomycin, borrelidin, pristinamycin, kanamycin, desferrioxamin, and melanin (Hu et al. 2018). However, only desferrioxamin and melanin were identified in the crude extract using LC-MS analysis. Desferrioxamin and melanin biosynthesis clusters of *S. parvulus* SX6 had a high homology (≥ 60%) to the existing clusters available in AntiSMASH database. These clusters were previously shown to be associated with antioxidant and anticancer activities (El-Naggar and El-Ewasy 2017; Hu et al. 2018). In contrast, friulimicin, lobophorin, laspartomycin, colabomycin, borrelidin, pristinamycin, and kanamycin clusters were not predicted in the SX6 genome. It leads to speculation that despite being classified into the same species, the BGCs can differ due to environmental niche adaptations.

Genomic analysis of *S. parvulus* SX6 revealed clusters 2 and 20 with moderate to low similarities with the cluster of actinomycin D known as a highly effective chemotherapeutic and antimicrobial agents (Khieu et al. 2015; Cai et al. 2016; Liu et al. 2016). In soil-derived *S. parvulus*, actinomycin D cluster in *S. parvulus* 2297, but not JCM 4068, shared 82% similarity to the reference actinomycin D from *S. anulatus* available on AntiSMASH database. It suggested that clusters 2 and 20 of SX6 could be involved in synthesizing new secondary metabolites instead of actinomycin D.

In addition, clusters 19 and 25 were identified as hybrid BGCs with low similarities with streptovaricin and polyoxypeptin BGCs, respectively. Compared to the reference streptovaricin cluster, a structurally-related macrolide antibiotic with a cluster size around 95 kb comprising 41 open reading frames (Liu et al. 2020; Luo et al. 2022), cluster 19 contained duplicates of five genes encoding type I modular PKSs responsible for the streptovaricin backbone. Likewise, cluster 25 only contained core genes involved in the production of polyoxypeptin a potent apoptosis inducer (Balachandran et al. 2014). The genome-wide comparison revealed that streptovaricin was only predicted in the *S. parvulus* JCM 4068 genome, while *S. parvulus* 2297 genome comprised polyoxypeptin. At the phenotypic level, the SX6 extract showed selective activity against *P. aeruginosa* ATCC® 9027™ and MRSE ATCC® 35984™. In addition, compared to the cytotoxicity against the non-cancerous HEK-293 cell line, the SX6 extract exhibited more significant cytotoxicity towards A549, Hep3B, and MCF-7 cell lines. The substantial antibacterial and anticancer activities shown by *S. parvulus* SX6 could be related to BGCs 19 and 25. Since most BGCs remain inactive under normal laboratory fermentation conditions, analysis of secondary metabolites under different culture conditions would be a fascinating subject for future studies.

A highlight of this study was the presence of the biosynthetic pathways of plant-derived compounds, including daidzein and genistein. Daidzein and genistein are representative compounds of isoflavones found in plants, especially legumes (Sohn et al. 2021). Various *in vitro* and *in vivo* reports have described the beneficial effects of these compounds in treating human diseases such as cancer, pathogenic infection, cardiovascular conditions, and diabetic complications (Yamasaki et al. 2007; Liu et al. 2021; Sohn et al. 2021). Previous investigations demonstrated that these plant-derived compounds were only produced by a few endophytic actinobacteria such as *S. variabilis* LCP18, *S. cavourensis* YBQ59, and *Streptomyces* sp. SS52 (Vu et al. 2018; Nguyen et al. 2019a; Quach et al. 2021). In this study, nine homologous enzymes building complete daidzein and genistein pathways similar to that in plants were identified. It was partly in agreement with the biosynthesis of daidzein found in the genome of *Streptomyces* sp. SS52 (Nguyen et al. 2019b). Comparative analysis showed that most of these genes are conserved across *S. parvulus* species. It is worth noting that *huth* is duplicated in *S. parvulus* SX6, which may convert the phenylalanine to yield cinnamic acid. A recent study demonstrated that many duplicated genes, such as ABC transporters, contributed to fitness improvements of *Streptomyces albidoflavus* DEF1AK in planta conditions (Kunova et al. 2021). Thus, this finding supports the well-known assumption that gene duplication acts as a mechanism of genomic adaptation to a changing environment (Bratlie et al. 2010).

HPLC-DAD-MS analysis further confirmed the presence of daidzein and genistein in the SX6 extract. It inferred that these isoflavones might also contribute to antioxidant, antibacterial, and cytotoxic activities obtained in the *S. parvulus* SX6 extract. The current finding further highlighted the potential of *S. parvulus* as the producer of plant-derived compounds.

Conlusions

In this study, we reported for the first time a broad range of biological activities and the complete genome information for *S. parvulus* SX6 associated with *A. corniculatum. S. parvulus* SX6 showed significant inhibitory effects against bacterial pathogens, cancer cell lines, and free radicals. The genomic data comparison and analysis revealed the presence of 4 cryptic secondary metabolite BGCs likely contributing to observed bioactivities. In addition, the most significant finding represented here was the proposed biosynthetic pathways of plant-derived compounds such as daidzein and genistein. This study suggested that mangrove endophytic *S. parvulus* has the potential to produce novel metabolites and could be an effective platform for daidzein and genistein production.

ORCID
Quyet-Tien Phi https://orcid.org/0000-0002-7182-3384

Acknowledgements
The authors would like to thank the support of VAST – Culture Collection of Microorganisms, Institute of Biotechnology, Vietnam Academy of Science and Technology (www.vccm.vast.vn).

Funding
This study was financially supported by the Graduate University of Science and Technology, Vietnam Academy of Science and Technology under grant number GUST.STS.ĐT2020-SH04 and Vietnam Academy of Science and Technology under grant number ĐLTE00.03/21-22.

Conflict of interest
The authors do not report any financial or personal connections with other persons or organizations, which might negatively affect the contents of this publication and/or claim authorship rights to this publication.

Literature

Andrews JM. Determination of minimum inhibitory concentrations. J Antimicrob Chemother. 2001 Jul;48(Suppl_1):5–16. https://doi.org/10.1093/jac/48.suppl_1.5

Aziz RK, Bartels D, Best AA, DeJongh M, Disz T, Edwards RA, Formsma K, Gerdes S, Glass EM, Kubal M, et al. The RAST server: rapid annotations using subsystems technology. BMC Genomics. 2008 Feb 8;9:75. https://doi.org/10.1186/1471-2164-9-75

Azman AS, Othman I, Fang CM, Chan KG, Goh BH, Lee LH. Antibacterial, anticancer and neuroprotective activities of rare actinobacteria from mangrove forest soils. Indian J Microbiol. 2017 Jun; 57(2):177–187. https://doi.org/10.1007/s12088-016-0627-z

Babicki S, Arndt D, Marcu A, Liang Y, Grant JR, Maciejewski A, Wishart DS. Heatmapper: web-enabled heat mapping for all. Nucleic Acids Res. 2016 Jul 8;44(W1):W147–W153. https://doi.org/10.1093/nar/gkw419

Balachandran C, Sangeetha B, Duraipandiyan V, Raj MK, Ignacimuthu S, Al-Dhabi NA, Balakrishna K, Parthasarathy K, Arulmozhi NM, Arasu MV. A flavonoid isolated from *Streptomyces* sp. (ERINLG-4) induces apoptosis in human lung cancer A549 cells through p53 and cytochrome c release caspase dependant pathway. Chem Biol Interact. 2014 Dec 5;224:24–35. https://doi.org/10.1016/j.cbi.2014.09.019

Bankevich A, Nurk S, Antipov D, Gurevich AA, Dvorkin M, Kulikov AS, Lesin VM, Nikolenko SI, Pham S, Prjibelski AD, et al. SPAdes: a new genome assembly algorithm and its applications to single-cell sequencing. J Comput Biol. 2012 May;19(5):455–477. https://doi.org/10.1089/cmb.2012.0021

Belknap KC, Park CJ, Barth BM, Andam CP. Genome mining of biosynthetic and chemotherapeutic gene clusters in *Streptomyces* bacteria. Sci Rep. 2020 Feb 6;10(1):2003. https://doi.org/10.1038/s41598-020-58904-9

Blin K, Wolf T, Chevrette MG, Lu X, Schwalen CJ, Kautsar SA, Suarez Duran HG, de Los Santos ELC, Kim HU, Nave M, et al. antiSMASH 4.0-improvements in chemistry prediction and gene cluster boundary identification. Nucleic Acids Res. 2017 Jul 3; 45(W1): W36–W41. https://doi.org/10.1093/nar/gkx319

Bolger AM, Lohse M, Usadel B. Trimmomatic: a flexible trimmer for Illumina sequence data. Bioinformatics. 2014 Aug 1;30(15): 2114–2120. https://doi.org/10.1093/bioinformatics/btu170

Bratlie MS, Johansen J, Sherman BT, Huang da W, Lempicki RA, Drabløs F. Gene duplications in prokaryotes can be associated with environmental adaptation. BMC Genomics. 2010 Oct 20;11:588. https://doi.org/10.1186/1471-2164-11-588

Cai W, Wang X, Elshahawi SI, Ponomareva LV, Liu X, McErlean MR, Cui Z, Arlinghaus AL, Thorson JS, Van Lanen SG. Antibacterial and cytotoxic actinomycins Y_6-Y_9 and Zp from *Streptomyces* sp. Strain Gö-GS12. J Nat Prod. 2016 Oct 28;79(10):2731–2739. https://doi.org/10.1021/acs.jnatprod.6b00742

Chandrakar S, Gupta AK. Actinomycin-producing endophytic *Streptomyces parvulus* associated with root of *Aloe vera* and optimization of conditions for antibiotic production. Probiotics Antimicrob Proteins. 2019 Sep;11(3):1055–1069. https://doi.org/10.1007/s12602-018-9451-6

Chevrette MG, Currie CR. Emerging evolutionary paradigms in antibiotic discovery. J Ind Microbiol Biotechnol. 2019 Mar;46(3–4): 257–271. https://doi.org/10.1007/s10295-018-2085-6

Chun J, Lee JH, Jung Y, Kim M, Kim S, Kim BK, Lim YW. EzTaxon: a web-based tool for the identification of prokaryotes based on 16S ribosomal RNA gene sequences. Int J Syst Evol Microbiol. 2007 Oct;57(Pt 10):2259–2261. https://doi.org/10.1099/ijs.0.64915-0

El-Naggar NA, El-Ewasy S. Bioproduction, characterization, anticancer and antioxidant activities of extracellular melanin pigment produced by newly isolated microbial cell factories *Streptomyces glaucescens* NEAE-H. Sci Rep. 2017 Feb 14;7:42129. https://doi.org/10.1038/srep42129

Galperin MY, Makarova KS, Wolf YI, Koonin EV. Expanded microbial genome coverage and improved protein family annotation in the COG database. Nucleic Acids Res. 2015 Jan;43(D1):D261–D269. https://doi.org/10.1093/nar/gku1223

Girão M, Ribeiro I, Ribeiro T, Azevedo IC, Pereira F, Urbatzka R, Leão PN, Carvalho MF. Actinobacteria isolated from *Laminaria ochroleuca*: a source of new bioactive compounds. Front Microbiol. 2019 Apr 9;10:683. https://doi.org/10.3389/fmicb.2019.00683

Holder IA, Boyce ST. Agar well diffusion assay testing of bacterial susceptibility to various antimicrobials in concentrations non-toxic for human cells in culture. Burns. 1994 Oct;20(5):426–429. https://doi.org/10.1016/0305-4179(94)90035-3

Hu D, Chen Y, Sun C, Jin T, Fan G, Liao Q, Mok KM, Lee MS. Genome guided investigation of antibiotics producing actinomycetales strain isolated from a Macau mangrove ecosystem. Sci Rep. 2018 Sep 24;8(1):14271. https://doi.org/10.1038/s41598-018-32076-z

Kadaikunnan S, Rejiniemon T, Khaled JM, Alharbi NS, Mothana R. *In-vitro* antibacterial, antifungal, antioxidant and functional properties of *Bacillus amyloliquefaciens*. Ann Clin Microbiol Antimicrob. 2015 Feb 22;14:9. https://doi.org/10.1186/s12941-015-0069-1

Khieu TN, Liu MJ, Nimaichand S, Quach NT, Chu-Ky S, Phi QT, Vu TT, Nguyen TD, Xiong Z, Prabhu DM, et al. Characterization and evaluation of antimicrobial and cytotoxic effects of *Streptomyces* sp. HUST012 isolated from medicinal plant *Dracaena cochinchinensis* Lour. Front Microbiol. 2015 Jun 8;6:574. https://doi.org/10.3389/fmicb.2015.00574

Kunova A, Cortesi P, Saracchi M, Migdal G, Pasquali M. Draft genome sequences of two *Streptomyces albidoflavus* strains DEF1AK and DEF147AK with plant growth-promoting and biocontrol potential. Ann Microbiol. 2021;71:2. https://doi.org/10.1186/s13213-020-01616-2

Lee LH, Chan KG, Stach J, Wellington EMH, Goh BH. Editorial: The search for biological active agent(s) from Actinobacteria. Front Microbiol. 2018 May 1;9:824. https://doi.org/10.3389/fmicb.2018.00824

Liu J, Luo J, Ye H, Sun Y, Lu Z, Zeng X. Production, characterization and antioxidant activities *in vitro* of exopolysaccharides from endophytic bacterium *Paenibacillus polymyxa* EJS-3. Carbohydr Polym. 2009 Sep 05;78(2):275–281. https://doi.org/10.1016/j.carbpol.2009.03.046

Liu Q, Liu Y, Li G, Savolainen O, Chen Y, Nielsen J. *De novo* biosynthesis of bioactive isoflavonoids by engineered yeast cell factories. Nat Commun. 2021 Oct 19;12(1):6085. https://doi.org/10.1038/s41467-021-26361-1

Liu XF, Xiang L, Zhou Q, Carralot JP, Prunotto M, Niederfellner G, Pastan I. Actinomycin D enhances killing of cancer cells by immunotoxin RG7787 through activation of the extrinsic pathway of apoptosis. Proc Natl Acad Sci USA. 2016 Sep 20;113(38):10666–10671. https://doi.org/10.1073/pnas.1611481113

Liu YZ, Chen X, Li ZY, Huang LX, Sun YH. Ansavaricin J, a new heterocyclic ring-fused streptovaricin from gene stvP5-deleted mutant of *Streptomyces spectabilis* CCTCC M2017417. Chem Biodivers. 2020 Aug;17(8):e1900713. https://doi.org/10.1002/cbdv.201900713

Luo M, Dong Y, Tang L, Chen X, Hu Z, Xie W, Deng Z, Sun Y. Two new streptovaricin derivatives from mutants of *Streptomyces spectabilis* CCTCC M2017417. Nat Prod Res. 2022 Jul;36(14):3689–3694. https://doi.org/10.1080/14786419.2021.1881517

Meier-Kolthoff JP, Göker M. TYGS is an automated high-throughput platform for state-of-the-art genome-based taxonomy. Nat Commun. 2019 May 16;10(1):2182. https://doi.org/10.1038/s41467-019-10210-3

Moore BS, Hertweck C, Hopke JN, Izumikawa M, Kalaitzis JA, Nilsen G, O'Hare T, Piel J, Shipley PR, Xiang L, et al. Plant-like biosynthetic pathways in bacteria: from benzoic acid to chalcone. J Nat Prod. 2002 Dec;65(12):1956–1962. https://doi.org/10.1021/np020230m

Musa Z, Ma J, Egamberdieva D, Abdelshafy Mohamad OA, Abaydulla G, Liu Y, Li WJ, Li L. Diversity and antimicrobial potential of cultivable endophytic actinobacteria associated with the medicinal plant *Thymus roseus*. Front Microbiol. 2020 Mar 12;11:191. https://doi.org/10.3389/fmicb.2020.00191

Nguyen HV, Truong PM, Duong HT, Dinh HM, Nguyen CH. Genome sequence data of *Streptomyces* sp. SS52, an endophytic strain for daidzein biosynthesis. Data Brief. 2019a Nov 4;27:104746. https://doi.org/10.1016/j.dib.2019.104746

Nguyen QH, Nguyen HV, Vu TH, Chu-Ky S, Vu TT, Hoang H, Quach NT, Bui TL, Chu HH, Khieu TN, et al. Characterization of endophytic *Streptomyces griseorubens* MPT42 and assessment of antimicrobial synergistic interactions of its extract and essential oil from host plant *Litsea cubeba*. Antibiotics (Basel). 2019b Oct 28; 8(4):197. https://doi.org/10.3390/antibiotics8040197

Núñez-Montero K, Lamilla C, Abanto M, Maruyama F, Jorquera MA, Santos A, Martinez-Urtaza J, Barrientos L. Antarctic *Streptomyces fildesensis* So13.3 strain as a promising source for antimicrobials discovery. Sci Rep. 2019 May 16;9(1):7488. https://doi.org/10.1038/s41598-019-43960-7

Qian Z, Bruhn T, D'Agostino PM, Herrmann A, Haslbeck M, Antal N, Fiedler HP, Brack-Werner R, Gulder TAM. Discovery of the streptoketides by direct cloning and rapid heterologous expression of a cryptic PKS II gene cluster from *Streptomyces* sp. Tü 6314. J Org Chem. 2020 Jan 17;85(2):664–673. https://doi.org/10.1021/acs.joc.9b02741

Qin S, Li J, Chen HH, Zhao GZ, Zhu WY, Jiang CL, Xu LH, Li WJ. Isolation, diversity, and antimicrobial activity of rare actinobacteria from medicinal plants of tropical rain forests in Xishuangbanna, China. Appl Environ Microbiol. 2009 Oct;75(19):6176–6186. https://doi.org/10.1128/aem.01034-09

Quach NT, Nguyen QH, Vu THN, Le TTH, Ta TTT, Nguyen TD, Van Doan T, Van Nguyen T, Dang TT, Nguyen XC, et al. Plant-derived bioactive compounds produced by *Streptomyces variabilis* LCP18 associated with *Litsea cubeba* (Lour.) Pers as potential target to combat human pathogenic bacteria and human cancer cell lines. Braz J Microbiol. 2021 Sep;52(3):1215–1224. https://doi.org/10.1007/s42770-021-00510-6

Salam N, Khieu TN, Liu MJ, Vu TT, Chu-Ky S, Quach NT, Phi QT, Narsing Rao MP, Fontana A, Sarter S, et al. Endophytic actinobacteria associated with *Dracaena cochinchinensis* Lour.: isolation, diversity, and their cytotoxic activities. Biomed Res Int. 2017;2017: 1308563. https://doi.org/10.1155/2017/1308563

Seemann T. Prokka: rapid prokaryotic genome annotation. Bioinformatics. 2014 Jul 15;30(14):2068–2079. https://doi.org/10.1093/bioinformatics/btu153

Shetty PR, Buddana SK, Tatipamula VB, Naga YVV, Ahmad J. Production of polypeptide antibiotic from *Streptomyces parvulus* and its antibacterial activity. Braz J Microbiol. 2014 Apr 8;45(1):303–312. https://doi.org/10.1590/S1517-83822014005000022

Shrestha L, Marasini BP, Pradhan SP, Shrestha RK, Shrestha S, Regmi KP, Pandey BP. Biotransformation of daidzein, genistein, and naringenin by *Streptomyces* species isolated from high-altitude soil of Nepal. Int J Microbiol. 2021 Jun 19;2021:9948738. https://doi.org/10.1155/2021/9948738

Singh H, Kaur M, Jangra M, Mishra S, Nandanwar H, Pinnaka AK. Antimicrobial properties of the novel bacterial isolate *Paenibacillus* sp. SMB1 from a halo-alkaline lake in India. Sci Rep. 2019 Aug 9;9(1):11561. https://doi.org/10.1038/s41598-019-47879-x

Sohn SI, Pandian S, Oh YJ, Kang HJ, Cho WS, Cho YS. Metabolic engineering of isoflavones: an updated overview. Front Plant Sci. 2021 Jun 7;12:670103. https://doi.org/10.3389/fpls.2021.670103

Tan LT, Chan KG, Khan TM, Bukhari SI, Saokaew S, Duangjai A, Pusparajah P, Lee LH, Goh BH. *Streptomyces* sp. MUM212 as a source of antioxidants with radical scavenging and metal chelating properties. Front Pharmacol. 2017 May 17;8:276. https://doi.org/10.3389/fphar.2017.00276

Tian X, Zhang Z, Yang T, Chen M, Li J, Chen F, Yang J, Li W, Zhang B, Zhang Z, et al. Comparative genomics analysis of *Streptomyces* species reveals their adaptation to the marine environment and their diversity at the genomic level. Front Microbiol. 2016 Jun 27;7:998. https://doi.org/10.3389/fmicb.2016.00998

Vu HT, Nguyen DT, Nguyen HQ, Chu HH, Chu SK, Chau MV, Phi QT. Antimicrobial and cytotoxic properties of bioactive metabolites produced by *Streptomyces cavourensis* YBQ59 isolated from *Cinnamomum cassia* Prels in Yen Bai Province of Vietnam. Curr Microbiol. 2018 Oct;75(10):1247–1255. https://doi.org/10.1007/s00284-018-1517-x

Vu THN, Nguyen QH, Dinh TML, Quach NT, Khieu TN, Hoang H, Chu-Ky S, Vu TT, Chu HH, Lee J, et al. Endophytic actinomycetes associated with *Cinnamomum cassia* Presl in Hoa Binh province, Vietnam: distribution, antimicrobial activity and, genetic features. J Gen Appl Microbiol. 2020 Apr 13;66(1):24–31. https://doi.org/10.2323/jgam.2019.04.004

Vu THN, Quach NT, Nguyen NA, Nguyen HT, Ngo CC, Nguyen TD, Ho P-H, Hoang H, Chu HH, Phi QT. Genome mining associated with analysis of structure, antioxidant activity reveals the potential production of levan-rich exopolysaccharides by food-derived *Bacillus velezensis* VTX20. Appl Sci. 2021 Jul 30;11(15):7055. https://doi.org/10.3390/app11157055

Wang F, Xu M, Li Q, Sattler I, Lin W. *p*-Aminoacetophenonic acids produced by a mangrove endophyte *Streptomyces* sp. (strain HK10552). Molecules. 2010 Apr 16;15(4):2782–2790. https://doi.org/10.3390/molecules15042782

Williams ST, Goodfellow M, Alderson G, Wellington EM, Sneath PH, Sackin MJ. Numerical classification of *Streptomyces* and related genera. J Gen Microbiol. 1983 Jun;129(6):1743–1813. https://doi.org/10.1099/00221287-129-6-1743

Yamasaki M, Fujita S, Ishiyama E, Mukai A, Madhyastha H, Sakakibara Y, Suiko M, Hatakeyama K, Nemoto T, Morishita K, et al. Soy-derived isoflavones inhibit the growth of adult T-cell leukemia cells *in vitro* and *in vivo*. Cancer Sci. 2007 Nov;98(11):1740–1746. https://doi.org/10.1111/j.1349-7006.2007.00595.x

Yang Y, Yang X, Zhang Y, Zhou H, Zhang J, Xu L, Ding Z. A new daidzein derivative from endophytic *Streptomyces* sp. YIM 65408. Nat Prod Res. 2013;27(19):1727–1731. https://doi.org/10.1080/14786419.2012.750317

Supplementary materials are available on the journal's website.